

## ON UNIMODAL AND BIMODAL OPTIMAL DESIGN OF FUNICULAR ARCHES†

JAN BŁACHUT and ANTONI GAJEWSKI

The Institute of Physics, Technical University of Cracow, ul. Podchorążych 1, 30-084 Kraków, Poland

(Received 26 February 1979; in revised form 5 May 1980)

**Abstract**—The problem of determining the optimal cross-sectional area function of a funicular, transverse vibrating arches under external load and geometrical constraints is investigated by the use of Pontryagin maximum principle.

The unimodal formulation for optimal design of arches is discussed but in order to arrive at the correct optimal solution the bimodal formulation is introduced.

As an illustration the optimal design of a circular arch is provided in detail. The optimization with respect to the buckling load is also included.

### 1. INTRODUCTION

The attempts of determining the optimal shape of an elastic arch with respect to buckling received as yet are not satisfactory enough because:

(a) the solution obtained in paper [1] coincides with the first iteration of our results in the case of unimodal formulation only. That is why obtained shape of arch is not optimal;

(b) the buckling equations in paper [2] which might be received from the appropriate Rayleigh quotient for inextensional antisymmetrical buckling are too simplified (the fourth order of differential equations);

(c) the formulation itself of the optimal design of the arches with respect to buckling is not sufficient [1-4] because the papers mentioned concern only unimodal, i.e. the usual mathematical formulation for optimal design of arches against buckling, whereas bimodal formulation is in most cases necessary in order to arrive at the correct optimal solution (see below).

The bimodal optimization was introduced by Olhoff and Rasmussen [5], who considered the problem of maximizing the buckling load of a doubly clamped elastic column and indicated that unimodal (single) formulation is inadequate for the geometrically unconstrained optimization problem.

The optimal shape of column associated with the first (fundamental) critical load was not optimal with respect to the second critical load. Hence they formulated bimodal optimization problem which allowed them to find the optimal shape associated with both first and second form of buckling (for the same critical load). Clearly enough, we have there a degeneration of an eigenvalue, i.e. the critical force associated with two different deflection lines of the column.

A somewhat similar problem of optimal design of vibrating bar for one prescribed, fundamental frequency or simultaneously for two fixed, different frequencies was treated by Thermann [6].

This paper concerns the uni- and bimodal optimization of elastic, vibrating arches, as well as their optimization with regard to their stability.

### 2. ASSUMPTIONS, STATE EQUATIONS AND BOUNDARY CONDITIONS

In this work our attention is restricted (the same way as in Ref. [4]), to a linear elastic material, an inextensibility of arch centerline. The funicular state is also postulated.

Our state equations are based upon the six differential equations of motion, of the first order, and then solved numerically. Optimal solution will be obtained by the application of the Pontryagin's maximum principle, using an iterative procedure suggested by Grinev and Filipov [7].

We begin by considering the state equations (the equations of small vibrations of an arch),

†This paper was supported by Grant 05.12.

which we rewrite in the following set [4]:

$$\begin{aligned}
 \hat{v}' &= -k_0 \hat{w} \\
 \hat{w}' &= \hat{\varphi} \\
 \hat{\varphi}' &= M/EI - k_0^2 \hat{w} + k_0' \hat{v} \\
 \hat{M}' &= -\hat{K} + N_0 \hat{\varphi} \\
 \hat{K}' &= k_0 \hat{Z} + k_0^2 \hat{M} + (N_0' - p_{22}) \hat{\varphi} - (-N_0 k_0' + p_{11} - p_{22} k_0) \hat{v} \\
 &\quad - (N_0 k_0^2 + p_{12} + q_{22} k_0) \hat{w} + \rho A \hat{\ddot{w}} \\
 \hat{Z}' &= -k_0' \hat{M} - (q_{11} - q_{22} k_0) \hat{v} - (q_{12} - q_{22}') \hat{w} + \rho A \hat{\ddot{v}},
 \end{aligned} \tag{1}$$

where: primes and dots denote differentiation with respect to  $s$  and  $t$  respectively;  $k_0 = -1/R(s)$ —the curvature of an arch in the undeformed state;  $E$ —Young's modulus;  $I(s)$ —the second moment of area of the cross-section;  $A(s)$ —the cross-sectional area;  $\rho(s)$ —the mass density;  $q_{ij}, p_{ij}$ —components which characterize the acting load during the motion of the structure [4];  $N_0$ —the compressive axial force;  $\hat{v}(s, t), \hat{w}(s, t)$ —the small displacements in the tangential and normal directions to the arch at the point  $s$ , caused by additional compressive force  $S$ .

The eqns (1) are obtained under the following notations:

$$\begin{aligned}
 \hat{\psi} &= -\hat{\varphi} + k_0 \hat{v} \\
 \hat{S} &= \hat{Z} + k_0 \hat{M} - q_{12} \hat{w} \\
 \hat{Q} &= \hat{K} - N_0 k_0 \hat{v},
 \end{aligned} \tag{2}$$

where  $\hat{\psi}$ —is an angle between tangent of the arch at the point  $s$  and the axis  $\xi$ ;  $\hat{S}, \hat{Q}$ —represent additional axial force and shear force respectively.

Introducing the following substitutions:

$$\begin{aligned}
 \hat{v} &= v \exp(i\omega t) & \hat{\varphi} &= \varphi \exp(i\omega t) \\
 \hat{w} &= w \exp(i\omega t) & \hat{K} &= K \exp(i\omega t) \\
 \hat{S} &= S \exp(i\omega t) & \hat{Z} &= Z \exp(i\omega t)
 \end{aligned} \tag{3}$$

we separate time and spatial variable, so that:

$$\begin{aligned}
 v' &= -k_0 w \\
 w' &= \varphi \\
 \varphi' &= M/EI - k_0^2 w + k_0' v \\
 M' &= -K + N_0 \varphi \\
 K' &= k_0 Z + k_0^2 M + (N_0' - p_{22}) \varphi - (-N_0 k_0' + p_{11} - p_{22} k_0) v \\
 &\quad - (N_0 k_0^2 + p_{12} + q_{22} k_0) w - \rho \omega^2 A w \\
 Z' &= -k_0' M - (q_{11} - q_{22} k_0) v - (q_{12} - q_{22}') w - \rho \omega^2 A v.
 \end{aligned} \tag{4}$$

To the state eqns (4) we add the appropriate boundary conditions according to the supporting mode. For instance: for a clamped-clamped arch we have:

$$\begin{aligned}
 v(0) &= 0 & w(0) &= 0 & \varphi(0) &= 0 \\
 v(1) &= 0 & w(1) &= 0 & \varphi(1) &= 0
 \end{aligned} \tag{5}$$

whereas for a hinged-hinged arch:

$$\begin{aligned} v(0) = 0 & \quad w(0) = 0 & \quad M(0) = 0 \\ v(1) = 0 & \quad w(1) = 0 & \quad M(1) = 0 \end{aligned} \quad (6)$$

### 3. FORMULATION OF THE UNIMODAL OPTIMIZATION PROBLEM

#### 3.1 Optimality criterion

The unimodal optimization problem will be now stated as follows. We are looking for such a function  $A(s)$  which minimize the total volume of an arch, i.e. we wish the following functional to be:

$$V = \int_0^1 A(s) ds \rightarrow \min \quad (7)$$

under the constraints:

(a) for the cross-section area

$$A_1 \leq A(s) \leq A_2 \quad (8)$$

(b) for the external load

$$p = \text{const} \quad (9)$$

(c) for the prescribed fundamental frequency of the transverse vibrations

$$\omega = \text{const.} \quad (10)$$

To investigate the problem (7)–(10) we apply formalism of the Pontryagin's maximum principle. The Hamiltonian connected with the state eqns (4) has the form:

$$H = \psi_v v' + \psi_w w' + \psi_\varphi \varphi' + \psi_M M' + \psi_K K' + \psi_Z Z' + \psi_0 A. \quad (11)$$

From (11) we obtain the following set of adjoint equations:

$$\begin{aligned} \psi'_v &= -\partial H/\partial v = -\psi_\varphi k'_0 + \psi_K(-N_0 k'_0 + p_{11} - p_{22} k_0) + \psi_Z(q_{11} - q_{22} k_0) + \psi_Z \rho \omega^2 A \\ \psi'_w &= -\partial H/\partial w = \psi_v k_0 + \psi_\varphi k_0^2 + \psi_K(N_0 k_0^2 + p_{12} + q_{22} k_0) + \psi_K \rho \omega^2 A + \psi_Z(q_{12} - q'_{22}) \\ \psi'_\varphi &= -\partial H/\partial \varphi = -\psi_w - N_0 \psi_M - \psi_K(N'_0 - p_{22}) \\ \psi'_M &= -\partial H/\partial M = -\psi_\varphi EI - \psi_K k_0^2 + \psi_Z k'_0 \\ \psi'_K &= -\partial H/\partial K = \psi_M \\ \psi'_Z &= -\partial H/\partial Z = -\psi_K k_0. \end{aligned} \quad (12)$$

Assuming the notation:

$$\psi_v = -\bar{Z}; \quad \psi_Z = \bar{v}; \quad \psi_\varphi = -\bar{M}; \quad \psi_K = \bar{w}; \quad \psi_w = -\bar{K}; \quad \psi_M = \bar{\varphi} \quad (13)$$

the adjoint system (12) can be written in the form:

$$\begin{aligned} \bar{Z}' &= -k'_0 \bar{M} + (N_0 k'_0 - p_{11} + p_{22} k_0) \bar{w} - (q_{11} - q_{22} k_0) \bar{v} - \rho \omega^2 A \bar{v} \\ \bar{K}' &= k_0 \bar{Z} + k_0^2 \bar{M} - (N_0 k_0^2 + p_{12} + q_{22} k_0) \bar{w} + (q_{12} - q'_{22}) \bar{v} - \rho \omega^2 A \bar{w} \\ \bar{M}' &= -\bar{K} + N_0 \bar{\varphi} + (N'_0 - p_{22}) \bar{w} \end{aligned}$$

$$\begin{aligned}\bar{\varphi}' &= \bar{M}/EI - k_0^2 \bar{w} + k_0' \bar{v} \\ \bar{w}' &= \bar{\varphi} \\ \bar{v}' &= -k_0 \bar{w}.\end{aligned}\tag{14}$$

To these equations we add a set of appropriate boundary conditions obtained from transversality conditions at  $s=0$  and  $s=1$ . It turns out that in some cases of loading the adjoint system might be reduced to the state equations. Then the boundary conditions of sets (4) and (14) are identical.

It means that then the set of state eqns (4) is selfadjoint. The conditions of selfadjointness of system (4) are:

$$\begin{aligned}(p_0 - q_{22})' - (p_{11} - q_{12}) &= 0 \\ N_0' - p_{22} &= 0.\end{aligned}\tag{15}$$

These conditions were derived in a different way by Farshad and Tadjbakhsh [4]. Relations (15) are satisfied for a circular arch under uniform normal pressure ( $p_0 = \text{const}$ ,  $N_0 = \text{const}$ ,  $p_{ij} = q_{ij} = 0$ ,  $i = j = 1, 2$ ), although such type of loading is, in fact, nonconservative, because the pressure has always the feature of tangential force. Fulfilment of (15) is caused only by the theory of funicular arches.

Generally speaking a necessary optimality condition leads to solution of the eqns (4) and (14) with the corresponding boundary conditions under assumption that the control function  $A(s)$  has to be determined from the upper-bound condition of the Hamiltonian with respect to  $A$ .

If in the whole range  $[A_1, A_2]$  the Hamiltonian  $H(A)$  is a convex function of  $A$  ( $H''_{AA} < 0$ ), then the optimal configuration, at a given point  $s$ , is a root  $A^*$  of the equation:

$$\partial H / \partial A = 0\tag{16}$$

—or is equal to that bound of an interval  $[A_1, A_2]$  which is closer to  $A^*$ .

On the other hand, if the Hamiltonian is a concave function of  $A$  ( $H''_{AA} > 0$ ), for all  $A \in [A_1, A_2]$ , then it reaches its maximum value for  $A_1$  or  $A_2$ .

### 3.2 Example—optimal design of a circular arch

Let us consider an elastic, plane, circular clamped-clamped arch ( $k_0 = -1/R = \text{const}$ ), of length 1, subjected to a hydrostatic pressure  $p_0$  (Fig. 1). We assume the cross-sections where area  $A(s)$  and the moment of inertia  $I$  are correlated by  $I = cA^\nu$ , with the constant  $\nu = 1, 2, 3$  in most frequent cases, i.e. for  $\nu = 1, 2, 3$  we get sandwich structures, geometrically similar cross-sections and rectangular beams of given width respectively.

In what follows we introduce the dimensionless quantities:

$$\begin{aligned}x &= s/1; \quad v^* = v/1; \quad w^* = w/1; \quad M^* = M/EI_0; \quad K^* = K I^2/EI_0 \\ \varphi^* &= \varphi; \quad Z^* = Z I^2/EI_0; \quad \beta = p_0 R^3/EI_0; \quad \Omega = \rho \omega^2 A_0 R^4/EI_0\end{aligned}\tag{17}$$

where  $I_0$  is the second moment of area of the cross-section at the point  $x_0$ , where the cross-sectional area is  $A_0$ . The point  $x_0$  is chosen in such a way as to satisfy the relation:

$$A_0 l = V.\tag{18}$$

So, introducing dimensionless cross-sectional area:

$$\phi(x) = A(x)/A_0\tag{19}$$

we get the following normalization condition for the cross-sectional area distribution:

$$\int_0^1 \phi(x) dx = 1\tag{20}$$

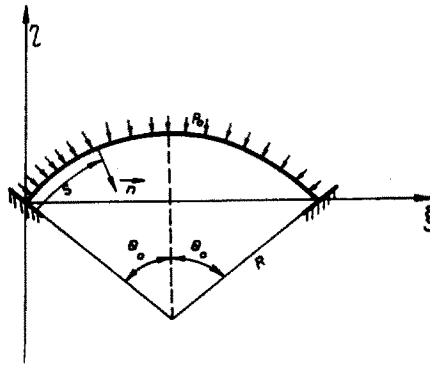


Fig. 1.

Substituting (17) and (19) into state eqns (4) we have:

$$\begin{aligned}
 v^{*'} &= \epsilon w^* \\
 w^{*'} &= \varphi^* \\
 \varphi^{*'} &= M^*/\phi^v - \epsilon^2 w^* \\
 M^{*'} &= -K^* - \epsilon^2 \beta \varphi^* \\
 K^{*'} &= -\epsilon Z^* + \epsilon^2 M^* + \epsilon^4 \beta w^* - \epsilon^4 \Omega \phi w^* \\
 Z^{*'} &= -\epsilon^4 \Omega \phi v^*
 \end{aligned}
 \tag{21}$$

where  $\epsilon = 1/R$  characterizes the steepness of the arch.

According to the method of solution applied, we reformulate the problem (7)–(19) as follows: we want to determine such a cross-sectional area function  $\phi(x)$ , under constraints:

$$\phi_1 \leq \phi \leq \phi_2 \tag{22}$$

$$\int_0^1 \phi(x) dx = 1 \tag{23}$$

$$\beta = \text{const} \tag{24}$$

which simultaneously satisfies state eqns (21) plus boundary conditions (5) and maximize a fundamental frequency of transversal vibrations, i.e.:

$$\Omega \rightarrow \text{max.} \tag{25}$$

In this case, there is also possibility of another formulation:

$$\beta \rightarrow \text{max,} \tag{26}$$

under the constraints: (22), (23), given  $\Omega = \text{const}$  with simultaneous satisfaction of the state eqns (21) plus boundary conditions (5).

The iterative method suggested in Ref. [7] may be used to find/starting from the formulation (7)–(10)/,  $\text{max } \Omega$  under  $\beta = \text{const}$ , as well as  $\text{max } \beta$ , under  $\Omega = \text{const}$ .

Let us consider the Hamiltonian  $H$  for the eqns (21):

$$\begin{aligned}
 H &= -Z^* \epsilon w^* - K^* \varphi^* - M^*(M^*/\phi^v - \epsilon^2 w^*) + \varphi^*(K^* + \epsilon^2 \beta \varphi^*) \\
 &+ w^*(-\epsilon Z^* + \epsilon^2 M^* + \epsilon^4 \beta w^* - \epsilon^4 \Omega \phi w^*) + v^*(-\epsilon^4 \Omega \phi v^*) - \lambda \phi.
 \end{aligned}
 \tag{27}$$

The optimality condition correlated with (16) leads to the following relation which determines  $\phi(x)$ :

$$\phi(x) = \left[ \frac{\nu M^{*2}}{\lambda + \epsilon^4 \Omega (v^{*2} + w^{*2})} \right]^{1/1+\nu} \quad (28)$$

where  $\lambda$  is the Lagrangian multiplier.

3.2.1 *The scheme of iterative procedure for optimal design connected with antisymmetric vibrations.* For numerical convenience we shall investigate two different forms of arch vibrations: symmetric and antisymmetric (Fig. 2). We are not able to say in advance which of them gives the first (the lowest) frequency as well as what is their relation in the process of arch optimization. That is reason why we shall optimize both symmetric and antisymmetric forms separately.

For clamped-clamped arches one may in a natural way distinguish the boundary conditions in the middle of an arch ( $x = 1/2$ ):

—antisymmetric vibrations:

$$\begin{aligned} v^*(0) = 0 & \quad w^*(0) = 0; & \quad \varphi^*(0) = 0; \\ w^*(1/2) = 0; & \quad M^*(1/2) = 0; & \quad Z^*(1/2) = 0; \end{aligned} \quad (29)$$

—symmetric vibrations:

$$\begin{aligned} v^*(0) = 0; & \quad w^*(0) = 0; & \quad \varphi^*(0) = 0; \\ v^*(1/2) = 0; & \quad \varphi^*(1/2) = 0; & \quad K^*(1/2) = 0. \end{aligned} \quad (30)$$

An iterative process in which we find maximal frequency for antimmetric form contains the following steps:

(a) for prescribed steepness of the arch  $\epsilon$ , pressure  $\beta$ , constraints  $\phi_1$  and  $\phi_2$  we assume at the beginning  $\phi(x) = 1.0$ ;

(b) we solve numerically the state eqns (21) with boundary conditions (29), converting two-point boundary value problem  $3 \times 3$  into an initial value problem which is solved by the use of a shooting-method;

(c) improved cross-section function  $\bar{\phi}_1(x)$  we get from:

$$\bar{\phi}_1(x) = \left[ \frac{\nu M^{*2}}{\lambda + \epsilon^4 \Omega_1^{(0)} (v^{*2} + w^{*2})} \right]^{1/1+\nu} \quad (31)$$

The constant  $\lambda$  should be calculated in accordance with (23). Than we substitute  $\bar{\phi}_1(x)$  into state equations from where we get the next value of  $\Omega_1^{(1)}$ , and the new, "improved" cross-section area function  $\bar{\phi}_2(x)$ .

The repetitions of introducing the improved cross-section area functions  $\bar{\phi}_i(x)$ , obtained each time from the optimality criteria (28) are going on until  $|\Omega_1^{(i)} - \Omega_1^{(i-1)}| < \delta$ , where  $\delta$  is an arbitrary small constant;  $i =$  number of iteration ( $i = 1, 2, \dots$ ). This process is quickly converged (in a few repetitions, sometimes even two,  $|\Omega_1^{(i)} - \Omega_1^{(i-1)}| / \Omega_1^{(i)}$  is less than 0.01). The same numerical procedure was successfully used by Grinev[8], but probably in the case of not selfadjoint systems of equations may not be converged.

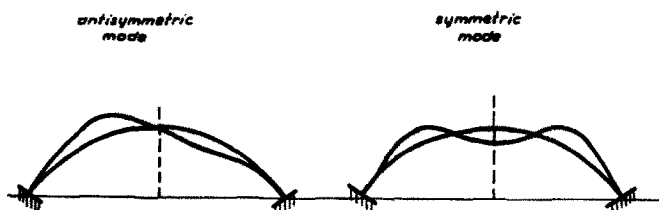


Fig. 2.

As a result of employed procedure we get  $\Omega_{1max}$  corresponding frequency to the optimal cross-section area function  $\phi_{opt}$ . Additionally, we only compute now the frequency of symmetric vibrations associated with  $\phi_{opt}$ , solving the state eqns (21) but this time taking into account the boundary conditions (30). It is done in order to find if accidentally the optimal arch with respect to antisymmetric vibrations has not the lower frequency of symmetric vibrations.

In Fig. 3 the relation between  $\beta_{max}$  and  $\Omega_{1max}^A$  is shown for the different constraints  $\phi_1$  subjected to the control variable  $\phi(x)$  at the antisymmetric vibrations.

An appropriate optimal cross-section area shape belongs to each point of the curves. For  $\beta_{max} \rightarrow 0$  we get maximum of the first (fundamental), natural frequency, while for  $\Omega_{1max}^A \rightarrow 0$  we get maximum of the lowest critical load  $\beta_{max}$ . For clarity we omit (at Fig. 3), curves associated with symmetric vibrations, which are lying above the antisymmetric ones, for the assumed constraints  $\phi_1$ .

3.2.2 *The scheme of iterative procedure for optimal design connected with symmetric vibrations.* To determine the optimal solution for symmetric vibrations we employ the same procedure of successive iterations as in Chapter 3.2.1, but introducing the boundary conditions (30) instead of (29). Then for the optimal shape we compute additionally the frequency of antisymmetric vibrations.

3.2.3 *Results and discussion of unimodal optimization.* As we have mentioned previously it is necessary to investigate both symmetric and antisymmetric vibrations. The full numerical procedure of successive iterations consists of the following steps:

- (a) the calculation of  $\phi_{opt}^A$  in  $i$ -iterations and  $\Omega_1^S$ ,
- (b) next, the calculation of  $\phi_{opt}^S$  in other  $j$ -iterations and appropriate  $\Omega_1^A$ .

In Figs. 4 and 5 some chosen results for different values of  $\beta$  and steepnesses  $\epsilon$  are shown. Solid curves  $\Omega_{1max}^A$  correspond to the maximal frequencies of antisymmetric vibrations as a function of the constraint  $\phi_1$ . The optimal shape  $\phi_{opt}^A$  belongs to each point of this lines (which isn't shown there).

Dashed lines represent the frequency of symmetric vibrations  $\Omega_1^S$  for optimal shapes  $\phi_{opt}^A$ . The same situation happens for the symmetric vibrations.

One might see that for some values of pressure (e.g. Fig. 5,  $\beta = 4$ ), the line  $\Omega_{1max}^A(\phi_1)$  represents optimal solution for any value of the constraint  $\phi_1$ . In this case the problem of maximization of the first (fundamental) frequency reduces to a discussion of the antisymmetric form of vibrations only. It does not however for  $\beta = 18$  (Fig. 5), where for  $\phi_1 < 0.41$  the arch of the optimal shape (maximizing the antisymmetric frequency), has the lower frequency of symmetric vibrations. Thus, the obtained solution for  $\phi_1 < 0.41$  is not optimal anymore. Nevertheless for some steepnesses, loadings and  $\phi_1$  the unimodal optimization is sufficient. But for  $\Omega_1 \rightarrow 0$ , i.e. in the

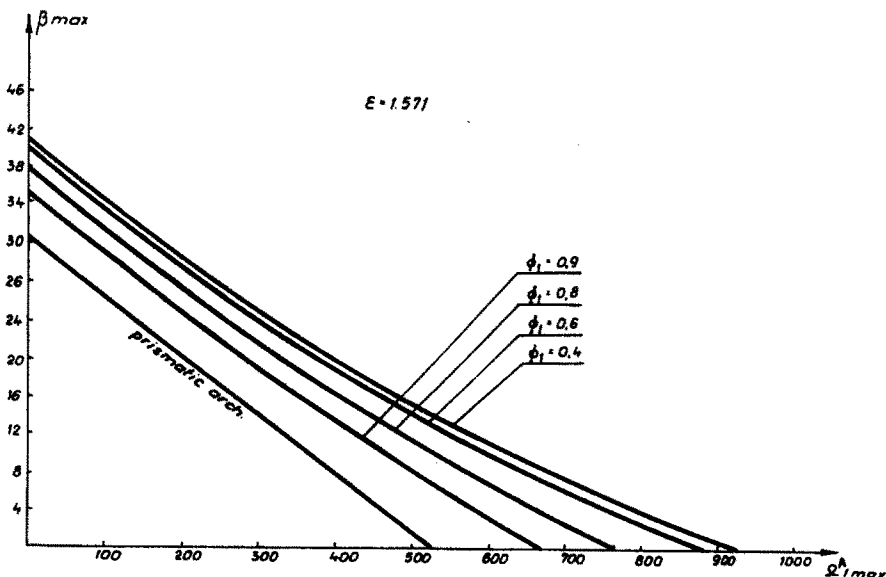
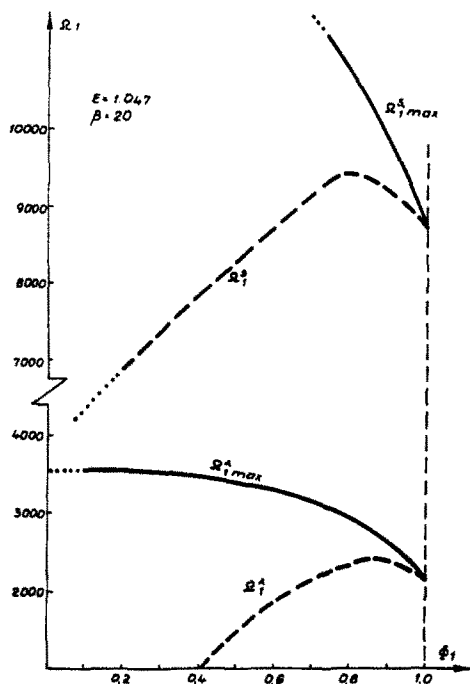
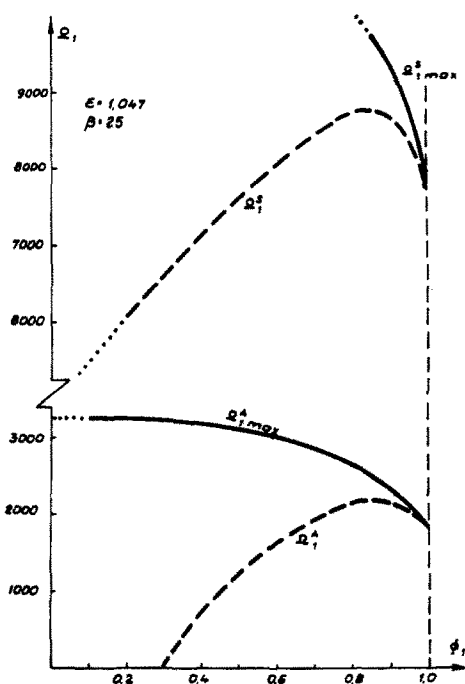


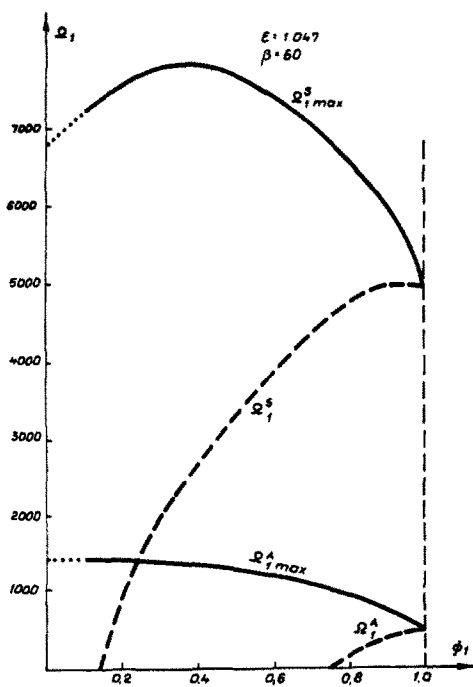
Fig. 3.



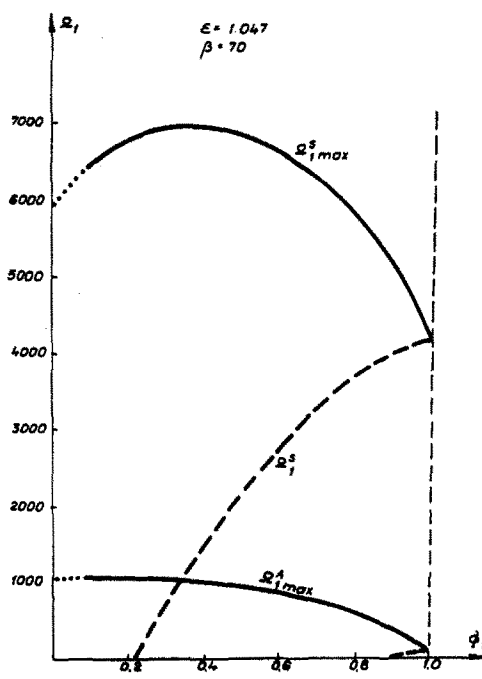
(a)



(b)



(c)



(d)

Fig. 4.



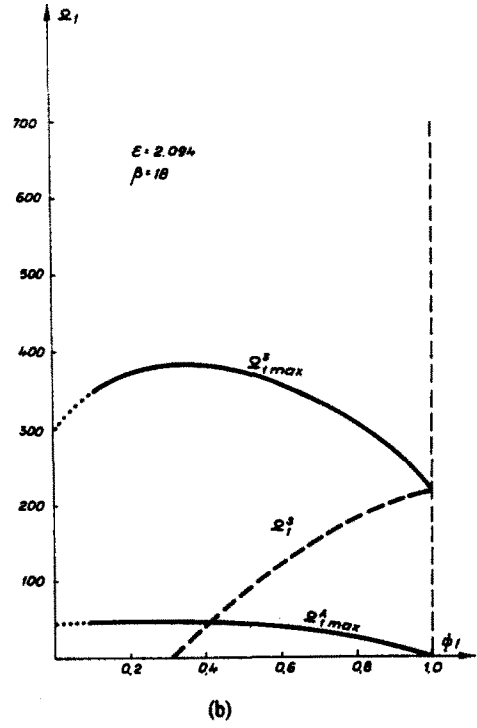
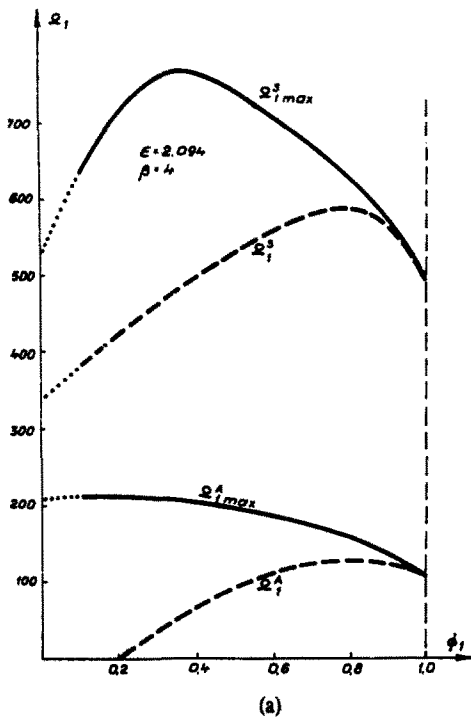


Fig. 5.

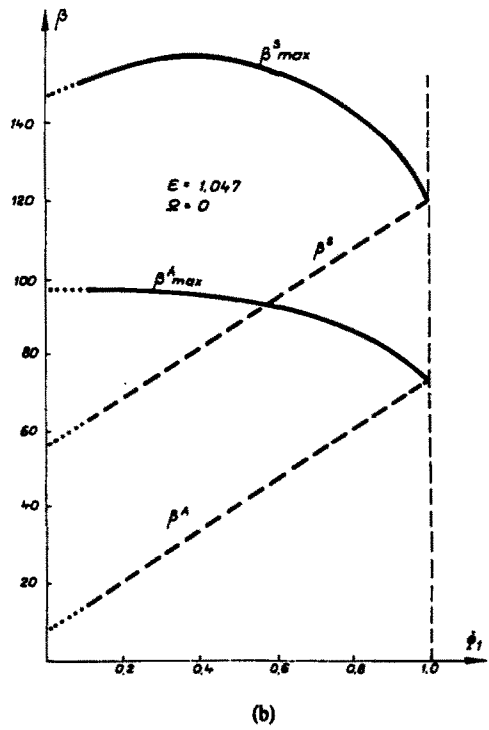
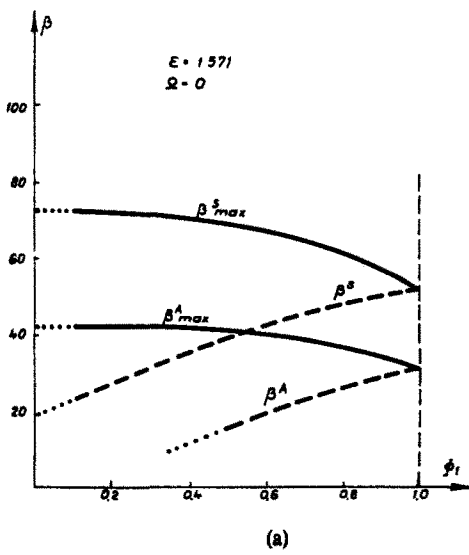


Fig. 6.

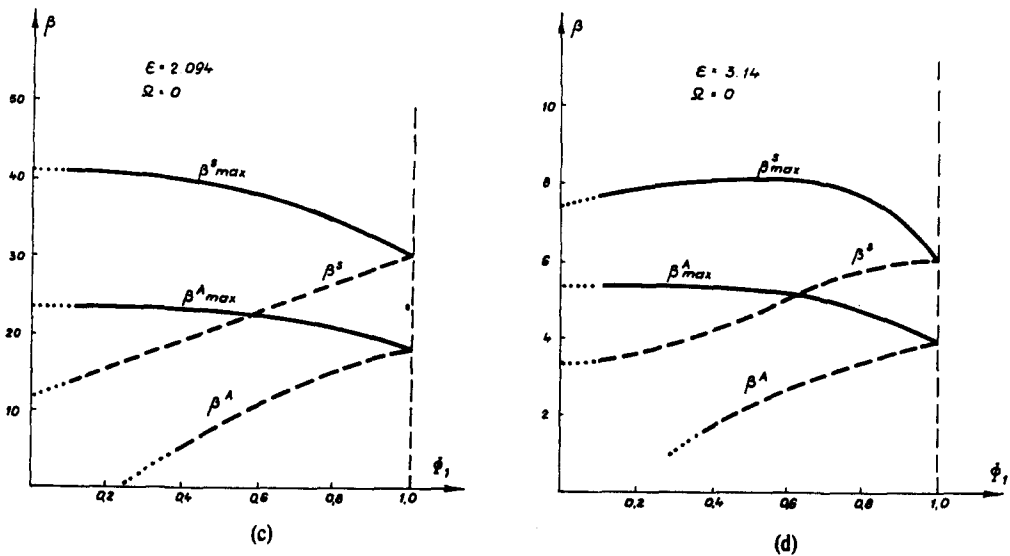


Fig. 6.

optimal design against buckling only, for  $1.047 \leq \epsilon \leq 3.141$  the unimodal optimization is not sufficient. It is illustrated in Fig. 6. In all four cases the optimal designed arch against buckling with respect to the antisymmetric form loses its stability at some value of constraint  $\phi_1$  with accordance to symmetric deflection line.

4. FORMULATION OF THE BIMODAL OPTIMIZATION PROBLEM

The optimization where both symmetric and antisymmetric forms are taken simultaneously into account we define as bimodal. Let us consider simultaneously symmetric and antisymmetric vibrations. Their differential equations have the following form:

$$\begin{aligned}
 v'_i &= -k_0 w_i \\
 w'_i &= \varphi_i \\
 \varphi'_i &= M_i/EI - k_0^2 w_i + k'_0 v_i \\
 M'_i &= -K_i + N_0 \varphi_i \\
 K'_i &= k_0 Z_i + k_0^2 M_i + (N'_0 - p_{22}) \varphi_i - (-N_0 k'_0 + p_{11} - p_{22} k_0) v_i \\
 &\quad - (N_0 k_0^2 + p_{12} + q_{12} k_0) w_i - \rho \omega_i^2 A w_i \\
 Z'_i &= -k'_0 M_i - (q_{11} - q_{22} k_0) v_i - (q_{12} - q'_{22}) w_i - \rho \omega_i^2 A v_i
 \end{aligned}
 \tag{32}$$

where  $i = 1, 2$ .

The form of vibrations is defined by appropriate boundary conditions:

—the antisymmetric vibrations ( $i = 1$ )

$$\begin{aligned}
 v_1(0) &= 0; & w_1(0) &= 0; & \varphi_1(0) &= 0; \\
 w_1(1/2) &= 0; & Z_1(1/2) &= 0; & M_1(1/2) &= 0;
 \end{aligned}
 \tag{33}$$

—the symmetric vibrations ( $i = 2$ )

$$\begin{aligned}
 v_2(0) &= 0; & w_2(0) &= 0 & \varphi_2(0) &= 0; \\
 v_2(1/2) &= 0; & \varphi_2(1/2) &= 0; & K_2(1/2) &= 0
 \end{aligned}
 \tag{34}$$

The Hamiltonian for the eqns (32) has the form of:

$$H = \sum_{i=1}^2 (\psi_{v_i} v'_i + \psi_{w_i} w'_i + \psi_{\varphi_i} \varphi'_i + \psi_{M_i} M'_i + \psi_{K_i} K'_i + \psi_{Z_i} Z'_i) + \psi_0 \phi$$

then the adjoint equations are the same as (12) with the addition of subscript "i" only.

Introducing again quantities, similarly as in (13) the adjoint equations have the same form as (14) with the addition of subscript “*i*” (*i* = 1, 2).

The optimality criterion is calculated on the basis of eqn (16).

4.1 Example—the circular arch

The state equations in the bimodal optimization process are the same as in Chapter 3.2.

Now the Hamiltonian is given by:

$$H = \sum_{i=1}^2 [\psi_{v_i} \epsilon w_i^* + \psi_{w_i} \phi_i^* + \psi_{\phi_i} (M_i^* / \phi^{\nu} - \epsilon^2 w_i^*) + \psi_{M_i} (-K_i^* - \epsilon^2 \beta \phi_i^*) + \psi_{K_i} (-\epsilon Z_i^* + \epsilon^2 M_i^* + \epsilon^4 \beta w_i^* - \epsilon^4 \Omega_i \phi w_i^*) + \psi_{Z_i} (-\epsilon^4 \Omega_i \phi v_i^*)] + \psi_0 \phi \tag{36}$$

With the use of notation (13), for *i* = 1, 2, and making use of the fact that the sets of the state equations and adjoint equations are seladjoint we obtain the optimal cross-sectional area distribution  $\phi$  if we employ the condition  $\partial H / \partial \phi = 0$ . Solving this equation with respect to  $\phi$  we find:

$$\phi(x) = \left[ \frac{\nu(M_1^{*2} + \mu M_2^{*2})}{\lambda + \epsilon^4 \Omega_1 (v_1^{*2} + w_1^{*2}) + \mu \epsilon^4 \Omega_2 (v_2^{*2} + w_2^{*2})} \right]^{1/(1+\nu)} \tag{37}$$

The formula (37) is identical with (28) if  $\mu$  tends to zero. The value of parameter  $\mu$  is a measure of contribution to the unimodal shape of another shape, i.e. we may “mix” both symmetric and antimmetric forms with different shares. The optimality condition (37) might be written in an equivalent form as follows†:

$$\phi(x) = \left\{ \frac{\nu[(1 - \bar{\mu})M_1^{*2} + \bar{\mu}M_2^{*2}]}{\lambda + (1 - \bar{\mu})\epsilon^4 \Omega_1 (v_1^{*2} + w_1^{*2}) + \bar{\mu}\epsilon^4 \Omega_2 (v_2^{*2} + w_2^{*2})} \right\}^{1/(1+\nu)} \tag{38}$$

This shape has the advantage of covering all possibilities as  $\bar{\mu}$  varies between zero and one. This formulation is symmetric and the limiting cases were investigated previously (see Figs. 4–6).

Using the optimality criterion (37) we apply the successive iterations method to get such optimal design variable  $\phi_{opt}$ , that  $\Omega_{1max} = \Omega_{2max}$  while  $\epsilon$ ,  $\beta$  and volume are prescribed. First we investigate the functions  $v_1^*$ ,  $w_1^*$ ,  $M_1^*$ , and eigenvalue  $\Omega_1$  integrating the state equations with boundary conditions (33) in the same way as it was done in the Chapter 3.2.1. On the contrary the functions  $v_2^*$ ,  $w_2^*$ ,  $M_2^*$  and eigenvalue  $\Omega_2$  we get integrating state equations with (34).

Next, we choose the parameter  $\mu$ . It is also done in an iterative way. Let the parameter  $\mu$  be  $\mu = \mu_1$  for which the optimal cross-section area distribution  $\bar{\phi}_1(x)$  has the same value of frequency for *i* = 1 and *i* = 2. In the next step, we solve state equations with boundary conditions (33) and (34). So, we obtain then:  $v_1^{*(1)}$ ,  $w_1^{*(1)}$ ,  $M_1^{*(1)}$ ,  $\Omega_1^{(1)}$ ,  $v_2^{*(1)}$ ,  $w_2^{*(1)}$ ,  $M_2^{*(1)}$ ,  $\Omega_2^{(1)}$ . Usually  $\Omega_1^{(1)}$  is different from  $\Omega_2^{(1)}$ . Next we calculate such a value of  $\mu$  which gives an improved shape  $\bar{\phi}_2^{(1)}$ . It should have the same value of symmetric and antimmetric frequencies (i.e. for *i* = 1 and *i* = 2).

Then again, we integrate state equations with (33) and (34) obtaining  $\Omega_1^{(i)}$  and  $\Omega_2^{(i)}$ . The search for  $\mu_i$  is going on until:

$$|\Omega_1^{(i)} - \Omega_2^{(i)}| < \delta_1 \tag{39}$$

where  $\delta_1$  is a small arbitrary constant.

If the relation (39) is obeyed, it means we found such a cross-section area distribution which has maximal, equal first and second frequencies.

For  $\epsilon = 1.047$  and  $\beta = 60, 65, 70$  as well as for  $\epsilon = 2.094$  and  $\beta = 18$  the relation between  $\Omega_{max}$  and  $\phi_1$  is plotted at Fig. 7. Meanwhile Fig. 8 shows the appropriate optimal cross-section area distribution.

†The formula (38) was suggested by a reviser of this paper.

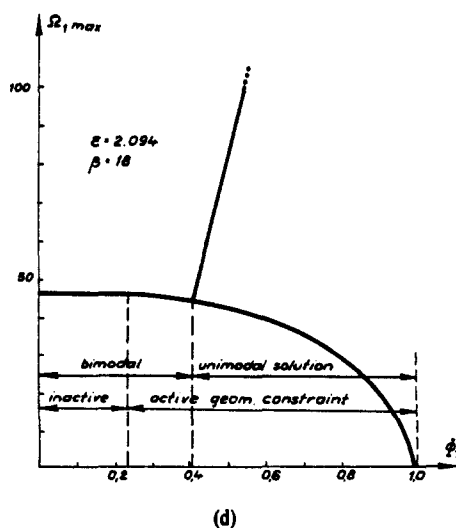
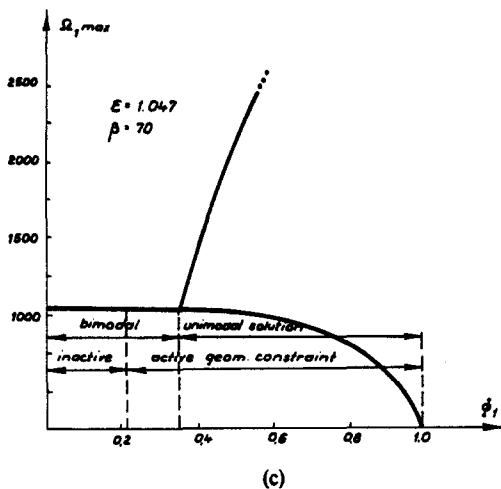
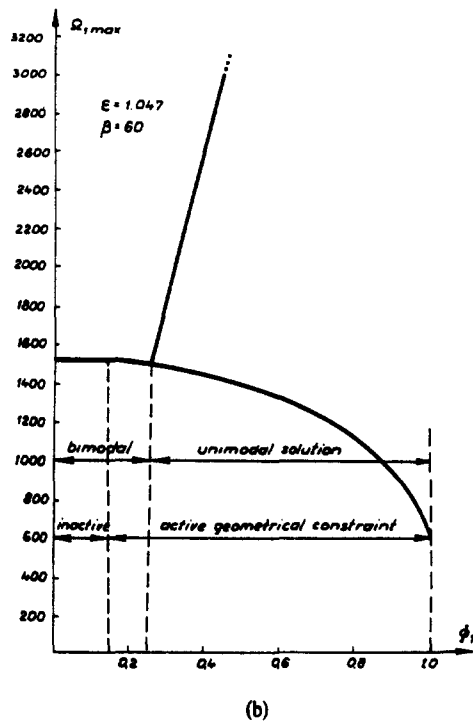
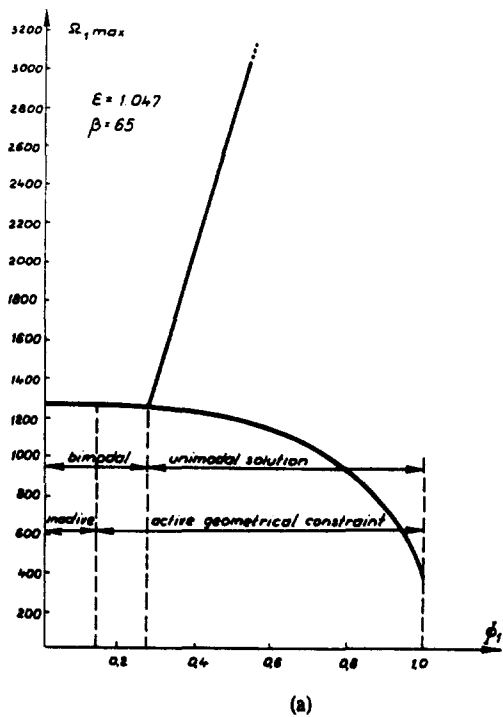


Fig. 7.

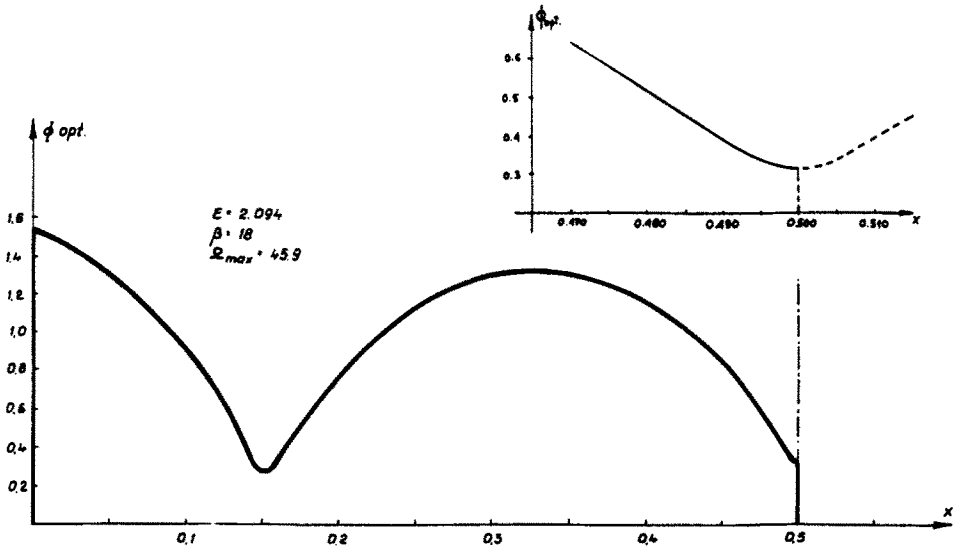


Fig. 8.

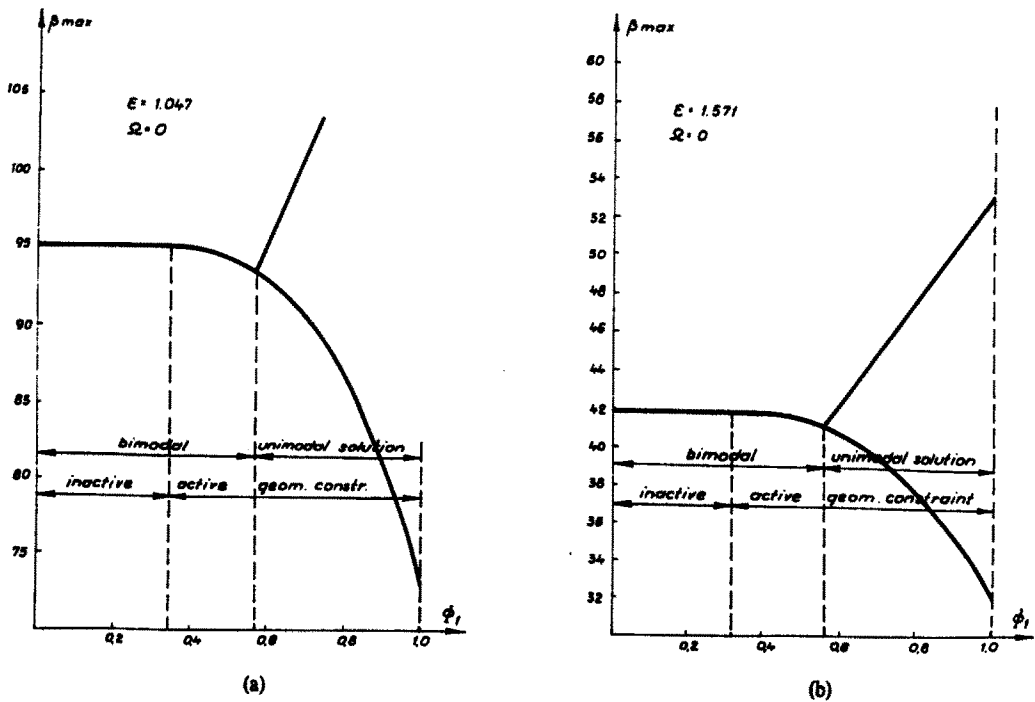
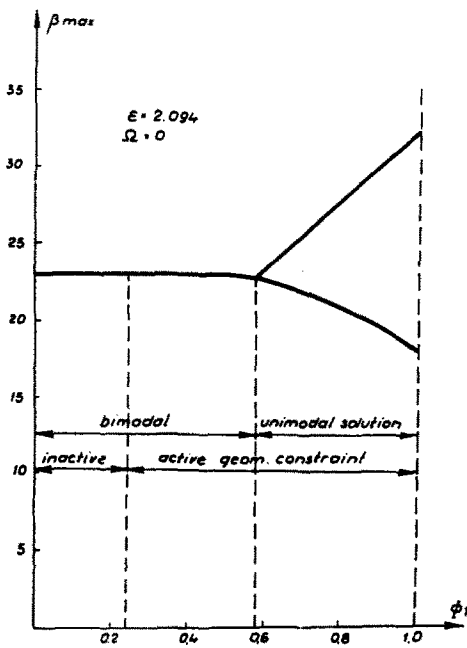
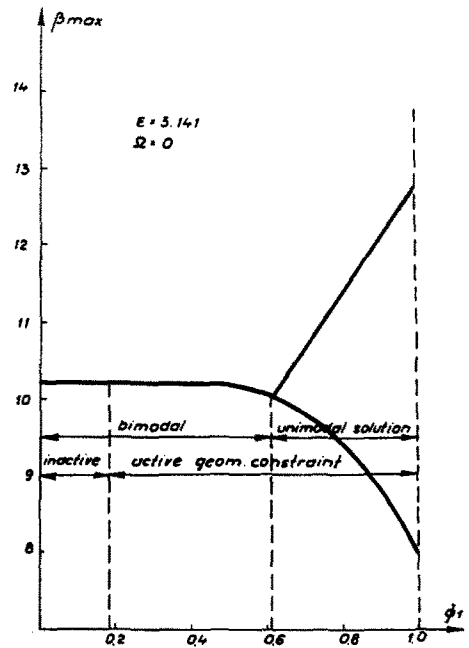


Fig. 9.



(c)



(d)

Fig. 9.

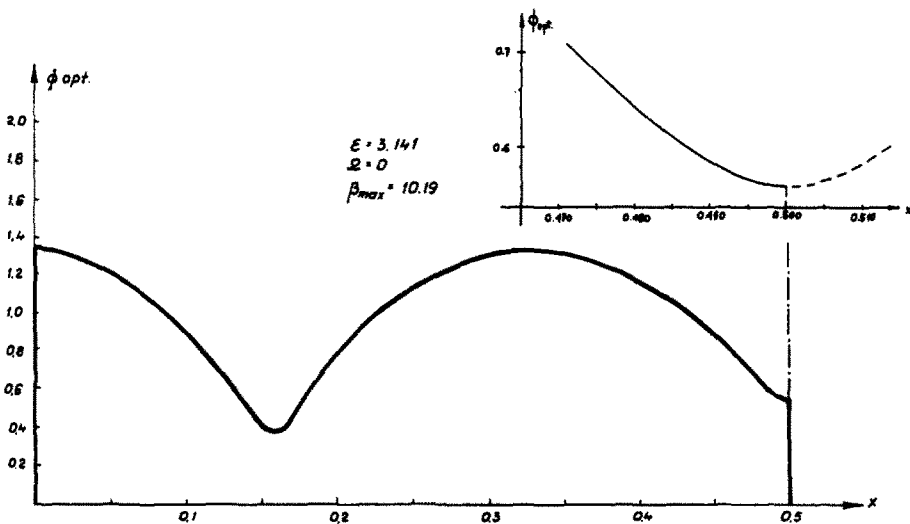


Fig. 10.

For several values of  $\epsilon$ , Fig. 9 shows the relation between  $\beta_{max}$  and  $\phi_1$  if  $\Omega$  tends to zero while at Fig. 10 the optimal cross-section area distribution of an arch for  $\epsilon = 3.141$  is shown.

5. CONCLUDING REMARKS

It should be noted that the optimal geometrically unconstrained cross-sectional area distribution of the arch against buckling obtained by the use of the unimodal formulation consists certain points where the optimal cross-section tends to zero. Obviously the unimodal formulation is insufficient in this case, whereas for any value of the constraint  $\phi_1$ , less than the threshold value, the optimal cross-sectional area distributions must be obtained with the use of the bimodal formulation. Moreover starting from a certain value of  $\phi_1$  the geometrical constraint became inactive.

So, the optimal shapes do not tend to zero anymore. We should finally remark that the Pontryagin's principle is an appropriate tool for investigation of the conservativeness conditions of loads.

*Acknowledgements*—The authors wish their thanks to Prof. M. Zyczkowski for his suggestions and helpful remarks through the work on this paper and to Dr. Z. Piekarski for discussion on it.

## REFERENCES

1. C. H. Wu, The strongest circular arch—a perturbation solution. *J. Appl. Mech.* 35(3), 476–480 (1968).
2. B. Budiansky, J. C. Frauenthal and J. W. Hutchinson, On optimal arches. *J. Appl. Mech.* 36(4), 880–882 (1969).
3. J. C. Amazigo, Optimal shape of shallow circular arches against snap-buckling. *J. Appl. Mech.* 45, 591–594 (1978).
4. I. Tadjbakhsh and M. Farshad, On conservatively loaded funicular arches and their optimal design. *IUTAM Symp. on Optimization in Structural Design*. Springer, Warsaw (1975).
5. N. Olhoff and S. H. Rasmussen, On single and bimodal optimum buckling loads of clamped columns. *Int. J. Solids Structures* 13, 605–614 (1977).
6. K. Thermann, Optimal design criteria of dynamically loaded elastic structures. *IUTAM Symp. on Optimization in Structural Design*. Springer, Warsaw (1975).
7. V. B. Grinev and A. P. Filipov, On optimal design of bars against buckling. *Stroit. Mekh. and Rasch. Sooruzh.* 2, 21–27 (1975).
8. V. B. Grinev, *Optimal Design of Structural Members*. (In Russian). Moscow (1975).